

Radiative transfer in the refractive atmospheres of very cool white dwarfs

P.M. Kowalski^{1,2} and D. Saumon^{2,1}

¹*Department of Physics and Astronomy, Vanderbilt University, Nashville, TN 37235-1807*

²*Los Alamos National Laboratory, MS F699, Los Alamos, NM 87545*

kowalski@lanl.gov

ABSTRACT

We consider the problem of radiative transfer in stellar atmospheres where the index of refraction departs from unity and is a function of density and temperature. We present modified Feautrier and Lambda-iteration methods to solve the equation of radiative transfer with refraction in a plane parallel atmosphere. These methods are general and can be used in any problem with 1-D geometry where the index of refraction is a monotonically varying function of vertical optical depth. We present an application to very cool white dwarf atmospheres where the index of refraction departs significantly from unity. We investigate how ray curvature and total internal reflection affect the limb darkening and the pressure-temperature structure of the atmosphere. Refraction results in a much weakened limb darkening effect. We find that through the constraint of radiative equilibrium, total internal reflection warms the white dwarf atmosphere near the surface ($\tau \lesssim 1$). This effect may have a significant impact on studies of very cool white dwarf stars.

Subject headings: radiative transfer – stars: atmospheres – stars: white dwarfs

1. Introduction

Problems involving radiative transfer in refractive media appear to have received limited attention (Harris 1965; Zheleznyakov 1967; Pomranin 1968). In stellar atmospheres in particular, refraction is always ignored since the gas is so tenuous that the index of refraction

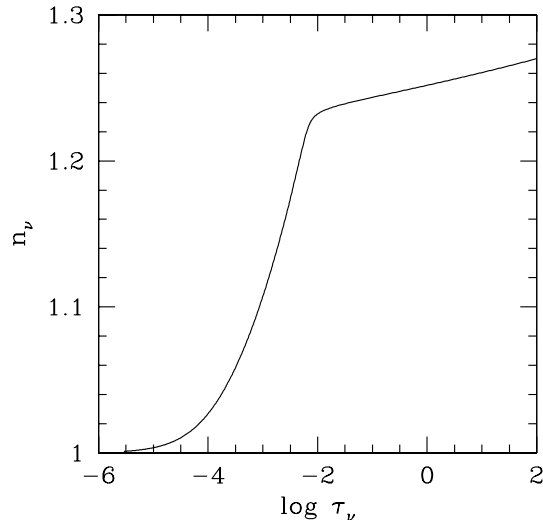


Fig. 1.— Variation of the index of refraction as a function of vertical optical depth τ_ν in the nominal white dwarf atmosphere model for $\lambda = 0.948 \mu\text{m}$.

does not depart from unity. A notable exception is found in the atmospheres of very cool white dwarfs, especially those rich in helium, where the gas (or rather the fluid) density can reach $0.1 - 2 \text{ g/cm}^3$. Under these conditions, the refractive index of fluid, atomic helium can become as large as ~ 1.3 with very large gradients (Fig. 1) and refraction can be expected to affect the radiation field. In this contribution, we study radiative transfer in a stellar atmosphere with refraction. While we are motivated primarily by astrophysical applications, the method developed here is general and can be directly applied to other problems with plane parallel geometry with an arbitrary, monotonic variation of the index of refraction.

We consider refraction in a stellar atmosphere that is static, plane parallel, in local thermal equilibrium, in hydrostatic equilibrium, with both radiative and convective energy transport. The total flux is constant throughout the atmosphere and scattering is assumed isotropic. We further assume that the refraction of ray paths follows Snell’s law (i.e. geometric optics) as is appropriate in white dwarf atmospheres. For a given run of the index of refraction through the atmosphere, this completely defines the trajectories of the ray paths and allows the derivation of a simple form of the equation of radiative transfer (ERT) in the presence of dispersive effects.

There is a number of interesting physical effects that we can expect in a stellar atmosphere where the index of refraction is greater than unity. The index n_ν is a monotonically

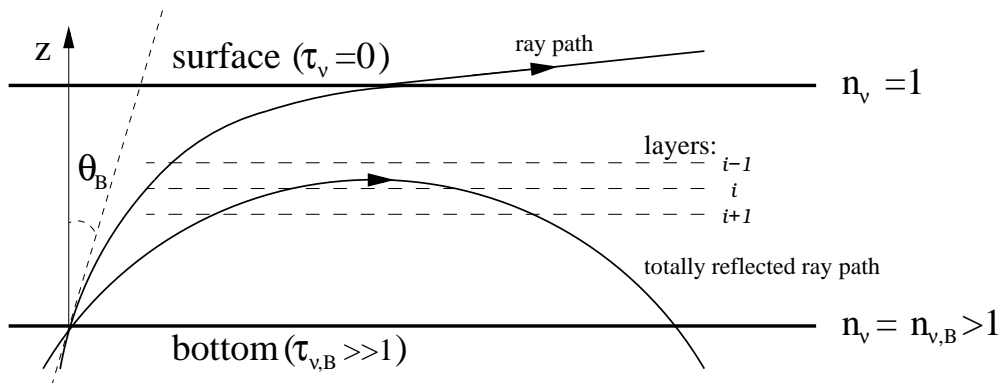


Fig. 2.— Geometry and typical ray paths for an axially symmetric radiation field in a refractive, planar atmosphere with a monotonically varying refractive index n_ν .

increasing function of density. In a stellar atmosphere, the index decreases from the bottom toward the surface where $n_\nu = 1$ at $\tau_\nu = 0$. All rays are refracted away from the upward vertical and some rays are internally reflected back toward the interior (Fig. 2). Intuitively, this should lead to an increase in the temperature profile of the atmosphere to achieve flux conservation. Because the largest variations of the index occur in the optically thin regions of the atmosphere (Fig. 1) we expect refraction to be mainly a surface effect. Furthermore, the group velocity of light is reduced by a factor of n_ν , so light accelerates toward the surface where it reaches the speed of light in a vacuum. This directly affects the flux through its dependence on the velocity of propagation. The angular redistribution of light due to refraction will reduce the limb darkening effect. Finally, the index of refraction of fluid helium is nearly independent of frequency from the optical to the near infrared and there should not be any significant chromatic effects.

We follow the treatment of the theory of radiative transfer in dispersive media presented by Cox & Giuli (1968). We develop two different numerical schemes to solve the ERT in the presence of refraction based on the Feautrier and Λ -iteration methods. Both methods are widely used in stellar atmosphere codes and the procedures we have developed allows for a straightforward implementation of the effects of refraction. To illustrate the effects of refraction in a stellar atmosphere, we apply both methods to solve for the radiation field in a realistic helium-rich white dwarf atmosphere model with $T_{\text{eff}} = 4000$ K, a gravity of $\log g(\text{cm/s}^2) = 8$ and a homogeneous composition of $n(\text{He})/n(\text{H}) = 10^6$, where $n(\text{X})$ is the number density of element X. This atmospheric structure, obtained with our white dwarf atmosphere code (Bergeron, Saumon & Wesemael 1995), is hereafter referred to as the “nominal” model.

In the next section, we construct the ERT for a refractive, planar atmosphere, and new expressions for the moments of the radiation field are given in Section 3. The numerical solution with modified Feautrier and Λ -iteration methods is described in Section 4. Numerical aspects of the solution, a detailed discussion of the effects of refraction on the radiation field, and the effects on the structure of the atmosphere and the emergent flux are presented in Section 5.

2. The equation of radiative transfer in the presence of refractive index gradient

The ERT along an arbitrary ray path is (Cox & Giuli 1968)

$$\frac{dI_\nu(\vec{r}, \vec{q})}{\rho ds} = j_\nu(\vec{r}, \vec{q}) - \chi_\nu(\vec{r}, \vec{q})I_\nu(\vec{r}, \vec{q}) + \left(\frac{dI_\nu(\vec{r}, \vec{q})}{\rho ds} \right)_{ref} \quad (1)$$

where I_ν is the specific intensity at point \vec{r} inside the atmosphere, \vec{q} is the direction of the curved ray path, ρ is the mass density, ds is an element along the curved ray path, j_ν is the total mass emission coefficient, and

$$\chi_\nu = \kappa_\nu + \sigma_\nu \quad (2)$$

is the total mass absorption coefficient, the sum of true absorption (κ_ν) and scattering (σ_ν) processes. The mass emission and absorption coefficients are related to their non-dispersive values j_ν^0 , χ_ν^0 by $j_\nu = n_\nu j_\nu^0$, and $\chi_\nu = \chi_\nu^0/n_\nu$, respectively (Harris 1965). The last term on the r.h.s. of Eq. (1) includes the contribution to $dI_\nu/\rho ds$ coming from spatial variations of the refractive index. In a horizontally homogeneous medium, the geometry leads to an axially symmetric radiation field. In the presence of refraction, the ray path is defined by Snell's law:

$$n_\nu \sin(\theta) = n'_\nu \sin(\theta') = \text{constant} \quad (3)$$

$$\phi = \phi' \pm \pi \quad (4)$$

where θ and ϕ are the polar angles coordinates with respect to the vertical z axis, parallel to the direction of the gradient of n_ν . Applying the law of energy conservation to an incident beam of radiation with solid angle $d\omega$, propagating from a medium with refractive index n_ν into a medium with refractive index n'_ν , and refracted into $d\omega'$,

$$I_\nu \cos(\theta)d\omega = I'_\nu \cos(\theta')d\omega' \quad (5)$$

we find that I_ν/n_ν^2 is constant along a ray path if there are no energy losses or gains due to emission, absorption, or interface effects (Cox & Giuli 1968). On the basis of that assumption, the last term in equation (1) is

$$\left(\frac{dI_\nu}{ds}\right)_{ref} = \frac{\partial I_\nu}{\partial n_\nu} \frac{dn_\nu}{ds} = \frac{2I_\nu}{n_\nu} \frac{dn_\nu}{ds} \quad (6)$$

and the ERT becomes

$$\frac{d}{\rho ds} \left(\frac{I_\nu(\vec{r}, \vec{q})}{n_\nu^2} \right) = \frac{j_\nu(\vec{r}, \vec{q}) - \chi_\nu(\vec{r}, \vec{q}) I_\nu(\vec{r}, \vec{q})}{n_\nu^2}. \quad (7)$$

In plane-parallel geometry, the derivative d/ds takes the form

$$\frac{d}{ds} = \cos \theta \frac{\partial}{\partial z} + \frac{d\theta}{ds} \frac{\partial}{\partial \theta}. \quad (8)$$

The derivative over θ appears because the ray paths are curved. For a given ray path, however, Eq. (3) allows us to reduce the configuration space from $\{z, \theta\}$ to a one-dimensional curve in $\{z\}$ only. The ray paths are parameterized by θ_B , the value of the ray path angle at a reference level chosen to be the bottom of the atmosphere (Fig. 2). Hereafter, all quantities with subscript “ B ” refer to this lower boundary. A ray path is described by

$$\mu_B = \cos \theta_B = \text{constant} \quad (9)$$

and as for each one dimensional curve $dz/ds = \cos \theta$, we can write

$$\frac{d}{ds} = \cos \theta \frac{\partial}{\partial z} \quad (10)$$

and rewrite the ERT (7) in a simpler form

$$\frac{\partial I'_\nu(\tau_\nu, \mu_B)}{\partial \sigma_\nu} = I'_\nu(\tau_\nu, \mu_B) - S'_\nu(\tau_\nu) \quad (11)$$

or

$$\mu(\mu_B, n(\tau_\nu)) \frac{\partial I'_\nu(\tau_\nu, \mu_B)}{\partial \tau_\nu} = I'_\nu(\tau_\nu, \mu_B) - S'_\nu(\tau_\nu), \quad (12)$$

where a primed quantity f' represents f/n_ν^2 , $S_\nu = j_\nu/\chi_\nu$ is the source function, σ_ν is now the optical depth measured along the curved ray path, τ_ν is the vertical optical depth, and

$$\mu = \text{sign}(\mu_B) \sqrt{1 - \left(\frac{n_{\nu,B}}{n_\nu}\right)^2 (1 - \mu_B^2)}. \quad (13)$$

The optical depths σ_ν and τ_ν are related to physical distances through the relations: $d\tau_\nu = -\rho\chi_\nu dz$ and $d\sigma_\nu = -\rho\chi_\nu ds$.

Equation (12) reduces to the well-known expression for the ERT for a non-refractive, plane-parallel atmosphere if we set $\mu = \text{constant}$ and $n_\nu = 1$. In the refractive case, however, the angle μ is now a function of μ_B and τ_ν , and at any given level, only the rays that started at the bottom with μ_B given by

$$\mu_{Bmin}^2(\tau_\nu) = 1 - \left(\frac{n_\nu(\tau_\nu)}{n_{\nu,B}} \right)^2 < \mu_B^2 < 1. \quad (14)$$

will not have been reflected downward. We label the set of all possible values of μ_B at a given τ_ν by ζ .

While Eqs. (11) and (12) are mathematically equivalent forms of the ERT, their numerical solution with finite difference schemes have very different accuracies for strongly curved ray paths. Equation (12) is simpler to solve numerically, as it does not require the calculation of σ_ν , however we find that it is essential to integrate the optical depth along the curved ray path to obtain a good solution and we will use the form given by Eq. (11).

3. Moments of the radiation field

The moments of the radiation field $J_\nu(\tau_\nu)$, $H_\nu(\tau_\nu)$, and $K_\nu(\tau_\nu)$ are defined as

$$J_\nu(\tau_\nu) = \frac{1}{2} \int_{-1}^1 I_\nu(\tau_\nu, \mu) d\mu, \quad (15)$$

$$H_\nu(\tau_\nu) = \frac{1}{2} \int_{-1}^1 \mu I_\nu(\tau_\nu, \mu) d\mu, \quad (16)$$

and

$$K_\nu(\tau_\nu) = \frac{1}{2} \int_{-1}^1 \mu^2 I_\nu(\tau_\nu, \mu) d\mu. \quad (17)$$

The ERT for the non-refractive case can be rewritten in terms of these moments:

$$\frac{\partial H_\nu(\tau_\nu)}{\partial \tau_\nu} = J_\nu(\tau_\nu) - S_\nu(\tau_\nu), \quad (18)$$

$$\frac{\partial K_\nu(\tau_\nu)}{\partial \tau_\nu} = H_\nu(\tau_\nu), \quad (19)$$

and

$$\frac{\partial^2 K_\nu(\tau_\nu)}{\partial \tau_\nu^2} = J_\nu(\tau_\nu) - S_\nu(\tau_\nu). \quad (20)$$

For the more general refractive case, the moments of the radiation field become

$$J'_\nu(\tau_\nu) = \frac{1}{2} \int_{-1}^1 I'_\nu(\tau_\nu, \mu) d\mu = \frac{1}{2} \int_{\zeta(\tau_\nu)} I'_\nu(\tau_\nu, \mu_B) \frac{\partial \mu}{\partial \mu_B} d\mu_B, \quad (21)$$

$$H'_\nu(\tau_\nu) = \frac{1}{2} \int_{-1}^1 \mu I'_\nu(\tau_\nu, \mu) d\mu = \frac{1}{2} \int_{\zeta(\tau_\nu)} \mu(\mu_B) I'_\nu(\tau_\nu, \mu_B) \frac{\partial \mu}{\partial \mu_B} d\mu_B, \quad (22)$$

and

$$K'_\nu(\tau_\nu) = \frac{1}{2} \int_{-1}^1 \mu^2 I'_\nu(\tau_\nu, \mu) d\mu = \frac{1}{2} \int_{\zeta(\tau_\nu)} \mu^2(\mu_B) I'_\nu(\tau_\nu, \mu_B) \frac{\partial \mu}{\partial \mu_B} d\mu_B, \quad (23)$$

where

$$\frac{\partial \mu}{\partial \mu_B} = \frac{\eta(\tau_\nu)}{\mu}, \quad (24)$$

and

$$\eta(\tau_\nu) = \mu_B \left(\frac{n_{v,B}}{n_\nu} \right)^2. \quad (25)$$

In the refractive case, J'_ν , H'_ν , and K'_ν are more convenient quantities than J_ν , H_ν and K_ν since I'_ν is constant along a ray path. The construction of the moments equations (18)–(20) is complicated by the fact that μ and the integration domain ζ are now functions of τ_ν . We first consider the derivative of H'_ν over τ_ν . For μ and η given by equations (13) and (25) we get

$$\frac{\partial \eta}{\partial \tau_\nu} = -2\eta \frac{1}{n_\nu} \frac{\partial n_\nu}{\partial \tau_\nu} \quad (26)$$

and

$$\frac{\partial \mu}{\partial \tau_\nu} = -\frac{1 - \mu^2}{\mu} \frac{1}{n_\nu} \frac{\partial n_\nu}{\partial \tau_\nu}. \quad (27)$$

Taking the derivative of (22) over τ_ν we obtain

$$\begin{aligned} \frac{\partial H'_\nu}{\partial \tau_\nu} &= \frac{1}{2} \frac{\partial}{\partial \tau_\nu} \int_{\zeta} \eta I'_\nu d\mu_B = \frac{1}{2} \int_{\zeta} \frac{\partial}{\partial \tau_\nu} (\eta I'_\nu) d\mu_B \\ &\quad - \frac{\partial \mu_{Bmin}}{\partial \tau_\nu} \eta I'_\nu \Big|_{\mu_B = \mu_{Bmin}} + \frac{\partial (-\mu_{Bmin})}{\partial \tau_\nu} \eta I'_\nu \Big|_{\mu_B = -\mu_{Bmin}}. \end{aligned} \quad (28)$$

Since $I'_\nu(\mu_{Bmin}) = I'_\nu(-\mu_{Bmin})$ and $\eta(\mu_{Bmin}) = -\eta(-\mu_{Bmin})$, we get

$$\begin{aligned} \frac{\partial H'_\nu}{\partial \tau_\nu} &= \frac{1}{2} \int_\zeta \frac{\partial}{\partial \tau_\nu} (\eta I'_\nu) d\mu_B \\ &= \frac{1}{2} \int_\zeta \frac{\partial \eta}{\partial \tau_\nu} (I'_\nu) d\mu_B + \frac{1}{2} \int_\zeta \eta \mu^{-1} (I'_\nu - S'_\nu) d\mu_B \\ &= J'_\nu - S'_\nu - 2H'_\nu \frac{1}{n_\nu} \frac{\partial n_\nu}{\partial \tau_\nu}, \end{aligned} \quad (29)$$

and finally

$$\frac{\partial H_\nu(\tau_\nu)}{\partial \tau_\nu} = J_\nu(\tau_\nu) - S_\nu(\tau_\nu), \quad (30)$$

which is identical to equation (18). The condition for radiative equilibrium

$$\frac{\partial}{\partial z} \int_0^\infty H_\nu d\nu = \int_0^\infty \chi_\nu (J_\nu - S_\nu) d\nu = 0 \quad (31)$$

remains unchanged. An analogous derivation for $\partial K'_\nu / \partial \tau_\nu$ gives

$$\frac{\partial K'_\nu}{\partial \tau_\nu} = H'_\nu(\tau_\nu) + \frac{1}{2} \int_\zeta \frac{\partial(\mu\eta)}{\partial \tau_\nu} I'_\nu d\mu_B - \frac{1}{2} \int_\zeta \eta S'_\nu d\mu_B. \quad (32)$$

Since η is antisymmetric in μ_B , the last term in equation (32) is 0 and we finally get

$$\frac{\partial K'_\nu}{\partial \tau_\nu} = H'_\nu(\tau_\nu) - (3K'_\nu - J'_\nu) \frac{1}{n_\nu} \frac{\partial n_\nu}{\partial \tau_\nu} \quad (33)$$

or

$$\frac{\partial K_\nu}{\partial \tau_\nu} = H_\nu(\tau_\nu) - (K_\nu - J_\nu) \frac{1}{n_\nu} \frac{\partial n_\nu}{\partial \tau_\nu}. \quad (34)$$

Equation (34) contains an additional term due to refraction. In cool white dwarf atmospheres, this term can dominate near the surface, as the gradient of the index of refraction becomes very large (Fig. 1). This equation may be used to evaluate the radiative flux H_ν when J_ν , K_ν , and n_ν are known. The form of Eq. (20) that includes refraction contains a term in $\partial J_\nu / \partial \tau_\nu$ and is not useful.

4. Solution of the equation of radiative transfer in a dispersive medium

4.1. Feautrier solution

In the presence of refraction, it remains advantageous to define the symmetric average of the specific intensity

$$P'(\mu_B, \nu, \sigma_\nu) = \frac{1}{2} [I'(\mu_B, \nu, \sigma_\nu) + I'(-\mu_B, \nu, \sigma_\nu)]. \quad (35)$$

Differentiating with respect to σ_ν , we obtain

$$\frac{\partial P'(\mu_B, \nu, \sigma_\nu)}{\partial \sigma_\nu} = \frac{1}{2}[I'(\mu_B, \nu, \sigma_\nu) - I'(-\mu_B, \nu, \sigma_\nu)] \quad (36)$$

and

$$\frac{\partial^2 P'(\mu_B, \nu, \sigma_\nu)}{\partial \sigma_\nu^2} = P'(\mu_B, \nu, \sigma_\nu) - S'(\sigma_\nu). \quad (37)$$

The source function in a dispersive medium and under the assumption of LTE and isotropic scattering is (Cox & Giuli 1968)

$$S'_\nu(\tau_\nu) = \epsilon_\nu B_\nu + (1 - \epsilon_\nu) J'_\nu, \quad (38)$$

where $\epsilon_\nu = \kappa_\nu/\chi_\nu$ is an absorption coefficient (equivalently, $1 - \epsilon_\nu$ is the scattering coefficient, or albedo). Equations (35–37) are mathematically identical to those used of the non-refractive case (Mihalas 1978), and their solution will require only minor changes.

Two boundary conditions are required to solve the second-order differential equation (37). At the bottom of the atmosphere, where $\tau_\nu \gg 1$, the radiation field is very close to thermodynamical equilibrium and

$$P'_B = B_\nu \quad (39)$$

where B_ν is the Planck function. To ease the notation, we drop the subscript ν in the remainder of our discussion of the solution of the ERT (Eqs. 39 – 51).

We consider that there is no incident radiation on the top of the atmosphere ($\tau_\nu = 0$). For ray paths that exit at the surface ($\mu_B > \mu_{Bmin}(0)$), the surface boundary condition is obtained from Eqs. (35) and (36):

$$\left. \frac{\partial P'}{\partial \sigma} \right|_{\sigma_{surface}} = P'_0. \quad (40)$$

Because of refraction, rays with $\mu_B < \mu_{Bmin}(0)$ are reflected downward (Fig. 2). These ray paths require a different boundary condition. At the reflection point, $\mu = 0$, $I'(+\mu) = I'(-\mu)$, and we have (36)

$$\left. \frac{\partial P'}{\partial \sigma} \right|_{\sigma_{reflection\ point}} = 0. \quad (41)$$

We solve the equations in finite difference form, where the vertical structure of the atmosphere is divided in $i = 1, 2, \dots, N$ horizontal layers with $i = 1$ corresponding to the topmost layer. We develop higher-order expressions for the boundary conditions using Taylor expansions:

$$P'_{i+1} = P'_i + \left. \frac{\partial P'}{\partial \sigma} \right|_{\sigma_i} \Delta\sigma_{i+1} + \frac{1}{2}(P'_i - S'_i)\Delta\sigma_{i+1}^2 \quad (42)$$

$$\left. \frac{\partial P'}{\partial \sigma} \right|_{\sigma_{top}} = \left. \frac{\partial P'}{\partial \sigma} \right|_{\sigma_i} + (P'_i - S'_i)(\sigma_{top} - \sigma_i) \quad (43)$$

where $\Delta\sigma_i = \sigma_i - \sigma_{i-1}$ and σ_{top} is the optical depth at the boundary (either the surface or the reflection point) measured along the ray path. For the surface boundary condition we get

$$\frac{P'_2 - P'_1}{\Delta\sigma_2} = P'_1 + \frac{1}{2}(P'_1 - S'_1)(\sigma_1 + \sigma_2 - 2\sigma_{top}) \quad (44)$$

and for the boundary condition for ray paths that are totally reflected between levels τ_R and τ_{R-1}

$$\frac{P'_{R+1} - P'_R}{\Delta\sigma_{R+1}} = \frac{1}{2}(P'_R - S'_R)(\sigma_R + \sigma_{R+1} - 2\sigma_{top}). \quad (45)$$

Equations (37), (39), (44), and (45) are solved by modifying the Feautrier solution (Mihalas 1978). The derivatives of any physical quantity f with respect to σ are evaluated with finite differences:

$$\left(\frac{df}{d\sigma} \right)_{i-\frac{1}{2}} = \frac{f_i - f_{i-1}}{\sigma_i - \sigma_{i-1}}, \quad (46)$$

and for the second derivative

$$\left(\frac{d^2 f}{d\sigma^2} \right)_i = \frac{\left(\frac{df}{d\sigma} \right)_{i+\frac{1}{2}} - \left(\frac{df}{d\sigma} \right)_{i-\frac{1}{2}}}{\frac{1}{2}(\sigma_{i+1} - \sigma_{i-1})}. \quad (47)$$

The ERT is solved on a discrete grid of μ_B points, that defines the ray paths. Each ray path is labeled $\mu_{B,k}$, where $k = 1, \dots, D$. The set of radiative transfer equations (37), can then be written as an algebraic matrix equation (Mihalas 1978):

$$-\mathbf{A}_i \mathbf{P}'_{i-1} + \mathbf{B}_i \mathbf{P}'_i - \mathbf{C}_i \mathbf{P}'_{i+1} = \mathbf{L}_i, \quad (48)$$

where \mathbf{A}_i , \mathbf{C}_i , and \mathbf{L}_i are $D \times 1$ vectors corresponding to layer i , with row $\{\mathbf{A}_i\}_j, \{\mathbf{C}_i\}_j, \{\mathbf{L}_i\}_j$ corresponding to ray path j , and \mathbf{B}_i is a $D \times D$ matrix, corresponding to layer i with elements $\{\mathbf{B}_i\}_{j,k=1,\dots,D}$ corresponding to ray path j . The surface and bottom boundary conditions are constructed from equations (44) and (39).

In the presence of refraction we need to consider the treatment of totally reflected ray paths. According to Eq. (45), for ray path j reflected between layers R and $R - 1$, the boundary condition for reflected rays can be written as

$$\sum_k \{\mathbf{B}_R\}_{j,k} \{\mathbf{P}'_R\}_k - \{\mathbf{C}_R\}_j \{\mathbf{P}'_{R+1}\}_j = \{\mathbf{L}_R\}_j. \quad (49)$$

Furthermore, the number of rays in a given layer decreases toward the top of the atmosphere. To maintain the dimensions of \mathbf{B}_i , the elements corresponding to reflected ray paths are

treated differently. For angles $\mu_{B,j} < \mu_{Bmin}(\tau_i)$, i.e. for ray paths reflected deeper than τ_i , we set:

$$\{\mathbf{B}_i\}_{j,k} = \begin{cases} 0, & \text{for } j \neq k \\ 1, & \text{for } j = k \end{cases} \quad (50)$$

and

$$\{\mathbf{A}_i\}_j = \{\mathbf{C}_i\}_j = \{\mathbf{L}_i\}_j = 0. \quad (51)$$

The solution of Eq. (47) for $P'(\tau_\nu, \mu_B)$ is otherwise identical to the non-refractive case (Mihalas 1978):

$$\begin{aligned} \mathbf{P}'_i &= \mathbf{D}_i \mathbf{P}'_{i+1} + \mathbf{v}_i \\ \mathbf{D}_i &= (\mathbf{B}_i - \mathbf{A}_i \mathbf{B}_{i-1})^{-1} \mathbf{C}_i \\ \mathbf{v}_i &= (\mathbf{B}_i - \mathbf{A}_i \mathbf{B}_{i-1})^{-1} (\mathbf{L}_i + \mathbf{A}_i \mathbf{v}_{i-1}) \\ \mathbf{D}_1 &= \mathbf{B}_1^{-1} \mathbf{C}_1 \\ \mathbf{v}_1 &= \mathbf{B}_1^{-1} \mathbf{L}_1, \end{aligned} \quad (52)$$

and the moments of the radiation field are then obtained with

$$J'_\nu(\tau_\nu) = \frac{1}{2} \int_0^1 P'_\nu(\tau_\nu, \mu_B) d\mu, \quad (53)$$

$$H'_\nu(\tau_\nu) = \frac{1}{2} \int_0^1 \mu^2 \frac{\partial P'_\nu(\tau_\nu, \mu_B)}{\partial \tau_\nu} d\mu = \frac{1}{2} \int_0^1 \mu \frac{\partial P'_\nu(\sigma_\nu, \mu_B)}{\partial \sigma_\nu} d\mu, \quad (54)$$

and

$$K'_\nu(\tau_\nu) = \frac{1}{2} \int_0^1 \mu^2 P'_\nu(\tau_\nu, \mu_B) d\mu. \quad (55)$$

4.2. Λ -iteration method

Given the formal solution of the ERT along a ray path between optical depths $\sigma_{\nu,1}$ and $\sigma_{\nu,2}$ ($\sigma_{\nu,1} < \sigma_{\nu,2}$)

$$I'_\nu(\sigma_{\nu,1}) = I'_\nu(\sigma_{\nu,2}) e^{-(\sigma_{\nu,2} - \sigma_{\nu,1})} + \int_{\sigma_{\nu,1}}^{\sigma_{\nu,2}} S'_\nu(t) e^{-(t - \sigma_{\nu,1})} dt, \quad (56)$$

the mean intensity (21) is given by

$$J'_\nu(\tau_\nu) = \frac{1}{2} \int_{-1}^1 I'_\nu(\sigma_\nu(\tau_\nu)) d\mu = \Lambda[S'_\nu(t)], \quad (57)$$

where Λ is an operator which acts on the source function S'_ν . The source function (38) is

$$S'_\nu(\tau_\nu) = \epsilon_\nu B_\nu + (1 - \epsilon_\nu)\Lambda[S'_\nu(t)]. \quad (58)$$

An iterative method can be used to find the value of the source function S'_ν at a given atmosphere level

$$S'_{l+1} = \epsilon_\nu B_\nu + (1 - \epsilon_\nu)\Lambda S'_l. \quad (59)$$

This solution is known as the Λ -iteration method (Mihalas 1978). For a discrete grid of τ_ν points, Λ may also be represented as a matrix operator $\mathbf{\Lambda}$ that acts on the source function vector \mathbf{S}' (Olson & Kunasz 1987):

$$\mathbf{J}' = \mathbf{\Lambda S}'. \quad (60)$$

The elements of the matrix $\mathbf{\Lambda}$ depend only on the numerical scheme adopted for integrating over σ_ν and μ to evaluate the specific intensity I'_ν , and the mean intensity J'_ν , respectively. A good choice is to locally interpolate the source function by a quadratic expression in σ_ν , which allows for analytic integration in (56) and excellent numerical precision. In this case the construction of the $\mathbf{\Lambda}$ matrix is well-known and presented in details by Olson & Kunasz (1987). Once the source function S'_ν is obtained by solving (59), I'_ν is computed from (56), and the moments J'_ν , H'_ν and K'_ν follow by direct integration. For the Λ -iteration procedure, the boundary conditions are physically the same as in the non-refractive case: 1) $I'_\nu = B_\nu$ at the bottom of the atmosphere and 2) there is no incident radiation at the surface $I'_\nu(\mu < 0) = 0$. There is no need for a “surface” boundary condition for the totally reflected ray paths. Since the Λ -iteration method solves directly for I'_ν , we can integrate along the full length of the reflected ray path (Eq. 56), including the downward part.

We found that the Λ -iteration method works very well for cool white dwarf atmospheres. However, it is well known that the Λ -iteration method converges poorly for nearly pure scattering media ($\epsilon_\nu \ll 1$) (Mihalas 1978). This difficulty can be circumvented with the accelerated Λ -iteration methods (ALI) (Cannon 1973; Olson, Auer & Buchler 1986; Hauschildt 1992; Hauschildt, Storzer & Baron 1993). Since the introduction of refraction does not affect the Λ -iteration method proper, the solution can be implemented just as easily with ALI as with the Λ -iteration.

5. Application to stellar atmospheres

5.1. Numerical considerations

As is usual, the atmosphere is divided vertically into discrete layers, $\tau_{\nu,i}$ (Fig. 2) and the ERT is solved for a finite set of ray paths $\mu_{B,k}$. Since in the refractive case the rays are no longer straight, the optical depth along the ray path σ_ν must be obtained by integration and it is related to the vertical optical depth τ_ν by

$$\sigma_\nu(\tau_\nu) = \int_{\tau_{0,\nu}}^{\tau_\nu} \frac{d\tau'_\nu}{\mu(\tau'_\nu)} \quad (61)$$

where $\tau_{0,\nu}$ is the optical depth at the bottom of the atmosphere for upward rays and $\tau_{0,\nu} = 0$ for downward rays that start from the surface. We found that it is essential to calculate σ_ν precisely along the curved ray paths. This is especially important in the layer where a given ray path is internally reflected. This is where the curvature of the ray is maximal and the ray can travel over a large horizontal distance (in optical depth) within that layer (Fig. 2). We locally interpolate $\mu(\tau_\nu)$ between τ_ν grid points with a quadratic polynomial to evaluate σ_ν analytically. To find the vertical optical depth τ_ν of the reflection point ($\mu(\tau_\nu) = 0$), we use Eq. (13) and a quadratic interpolation of $n_\nu(\tau_\nu)$. The integrals for the moments of the radiation field are performed numerically with a quadratic (3-point) integration scheme. The integration consists of two parts: $0 \leq \mu \leq \mu_c$ and $\mu_c \leq \mu \leq 1$, because $P'_\nu(\tau_\nu, \mu)$ is discontinuous at $\mu = \mu_c(\tau_\nu) = \sqrt{1 - n_\nu^2(\tau_\nu = 0)/n_\nu^2(\tau_\nu)}$ (see §5.2 below). Rays with $\mu < \mu_c(\tau_\nu)$ will be reflected before they reach the surface. In Eq. (56), $S'_\nu(\tau_\nu)$ is approximated by a quadratic polynomial in each layer (Olson & Kunasz 1987). The radiative flux from the Feautrier solution is calculated with both Eqs. (54) and (34) to check the numerical consistency of the solution.

We have verified that our methods of solutions and codes are correct in two ways. To check the consistency of the solutions obtained with the Feautrier and Λ -iteration methods, and their sensitivity to the resolution of the τ_ν and μ_B grids, we solved for the radiation field in a white dwarf atmosphere with a fixed (T, P) structure. This nominal structure corresponds to a non-refractive helium-rich model with $T_{\text{eff}} = 4000$ K, $\log g = 8$, $n(\text{He})/n(\text{H}) = 10^6$ in radiative/convective equilibrium. In this model the convection zone extends from the bottom of the atmosphere up to $\tau_R \sim 10^{-2}$. The input parameters for computing the radiation field are the refractive index $n_\nu(\tau_\nu)$ (Fig. 1), the absorption parameter $\epsilon_\nu(\tau_\nu)$ (Fig 3.), and the Planck function $B_\nu(\tau_\nu)$ (Fig 4.), all computed from the (T, P) structure.

For our most precise calculation, using $N = 500$ layers and $D = 500$ ray-paths, the relative differences between the two methods are smaller than 0.1% in both J_ν and H_ν , and

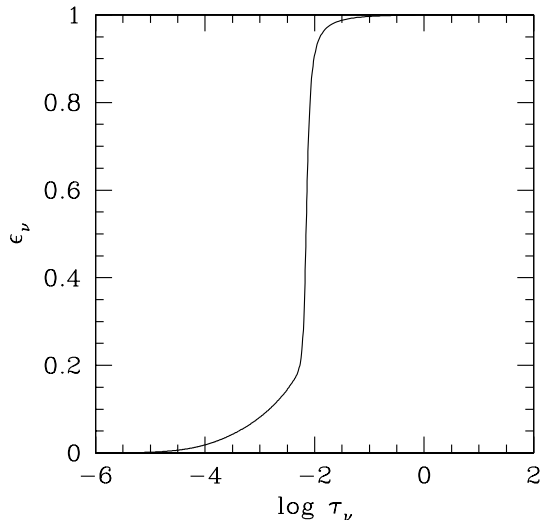


Fig. 3.— Absorption parameter $\epsilon_\nu = \kappa_\nu/\chi_\nu$ in the nominal white dwarf atmosphere model for $\lambda = 0.948 \mu\text{m}$. Pure scattering corresponds to $\epsilon_\nu = 0$.

the internal precision of both methods is better than 0.01%. The difference between the two solutions decreases significantly as the number of layers increases. With 50 layers, the moments of the radiation field can differ by as much as 1%. On the other hand, the solution is much less sensitive to the number of ray paths. In situations where the optical thickness of a layer $\tau_{\nu,i+1} - \tau_{\nu,i} \gtrsim 1$, as is common in the deeper region of atmosphere models, the application of a quadratic interpolation of the source function S'_ν in Eq. (56) is more precise than the solution of Eq. (37) using a finite difference scheme. The Λ -iteration method is therefore a better choice when computing a model with a relatively small number of layers ($N \sim 50$).

We have also compared with published solutions to a similar but simpler problem, where radiative transfer with refraction is considered in a dielectric slab (Abdallah & Dez 2000; Huang, Xia & Tan 2003). Both surfaces of the slab are maintained at fixed but different temperatures, radiative equilibrium is imposed, the index of refraction varies linearly between the two surfaces, and the absorption coefficient is constant. We note that Abdallah & Dez (2000) neglected the effect of dispersion on the absorption coefficient, assuming that $\kappa_\nu = \kappa_\nu^0$, while the correct expression is $\kappa_\nu = \kappa_\nu^0/n_\nu$, where κ_ν^0 is mass absorption coefficient in the absence of dispersive effects (Harris 1965). Setting $\kappa_\nu = \kappa_\nu^0$, we reproduce Figs. (3a–3c) of Abdallah & Dez (2000) perfectly. Introducing the effect of dispersion on κ_ν raises the temperature profile in the slab by a few degrees.

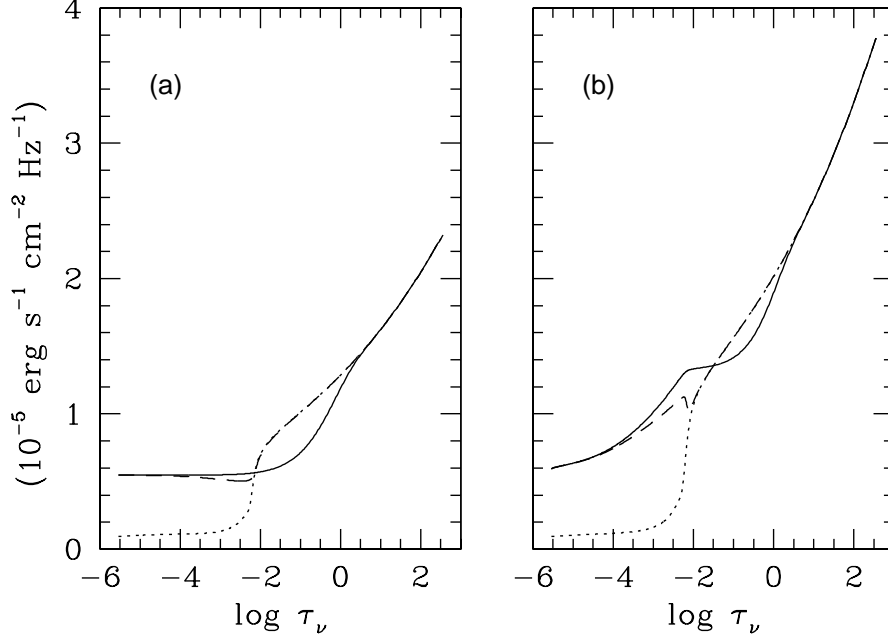


Fig. 4.— Mean intensity J_ν (solid line), source function S_ν (dashed line), and Planck function $n_\nu^2 B_\nu$ (dotted line) for non-refractive (a) and refractive (b) cases as a function of vertical optical depth τ_ν in the nominal white dwarf atmosphere model for $\lambda = 0.948 \mu\text{m}$.

5.2. Refraction inside white dwarf atmospheres

We now turn to a detailed discussion of the effects of refraction in our nominal white dwarf atmosphere model. Figure 4 shows the mean intensity, the source function and the Planck function for the refractive and non-refractive cases for the same nominal (T, P) structure. In the refractive case, J_ν increases by a factor of n_ν^2 at large optical depth because $J_\nu \sim S_\nu \sim n_\nu^2 B_\nu$ (Eq. 38). For $\tau_\nu < 10^{-2}$, $n_\nu \sim 1$ and $n_\nu^2 B_\nu \sim B_\nu$. However, J_ν remains significantly larger than in the non-refractive case because of total internal reflection. This can be understood from the angular distribution of the radiation. Figure 6 shows the angular distribution of the symmetric average of the specific intensity P'_ν for both cases at different levels in the atmosphere. Deep inside the atmosphere P'_ν is just the Planck function B_ν and it is the same in both cases. Toward the surface, P'_ν splits into two regions separated by a discontinuity at $\mu = \mu_c(\tau_\nu)$. The additional intensity for $\mu < \mu_c$ arises from the contribution of ray paths that have been reflected at lower τ_ν (above the level considered). Toward the

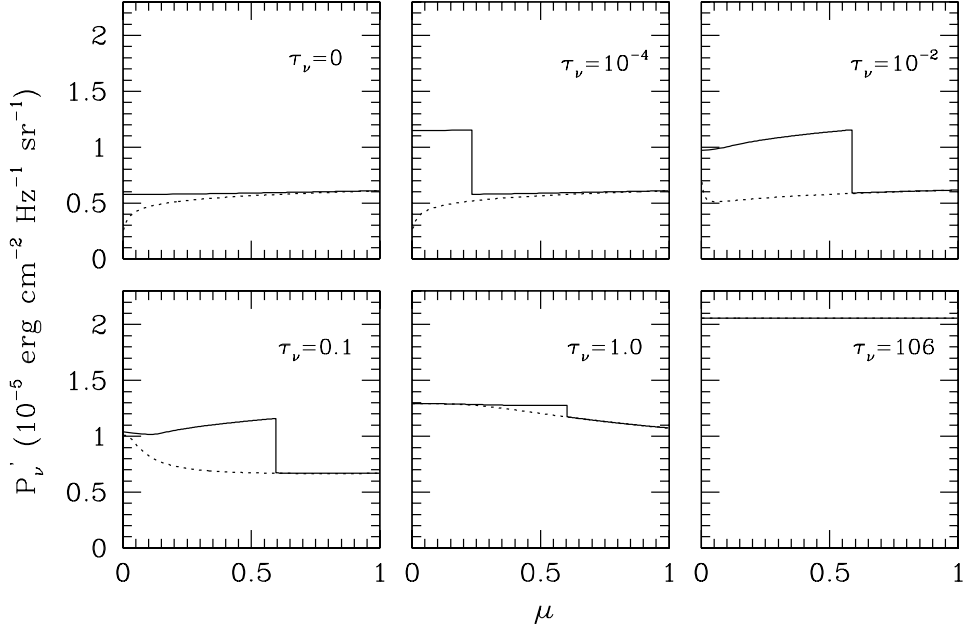


Fig. 5.— Symmetric average of the specific intensity $P'_\nu = P_\nu/n_\nu^2$ for refractive (solid line) and non-refractive (dotted line) cases as a function of angle $\mu = \cos\theta$ at various levels in the nominal white dwarf atmosphere model. $\mu = 0$ and 1 correspond to the horizontal and vertical directions, respectively. The wavelength is $\lambda = 0.948 \mu\text{m}$.

surface, P'_ν doubles across the discontinuity

$$P'_\nu(\mu_c^-) \sim 2P'_\nu(\mu_c^+) \quad (62)$$

because the contribution from the source function from the optically thin regions lying above for $\mu > \mu_c$ is negligible but the contribution from the downward rays ($\mu < 0$) that have been reflected higher up is nearly the same as for the upward rays ($\mu > 0$), due to negligible absorption-emission effects inside the optically thin region. This effect should result in warming of an atmosphere in radiative equilibrium, because an increase in the mean intensity J_ν must generally be compensated by an increase in the Planck function B_ν .

The angular distribution of the emergent radiation, known as limb darkening, is affected by refraction. Limb darkening is shown in the first panel of Fig. 6 since at $\tau = 0$, $P'_\nu(\mu) = P_\nu(\mu) = I_\nu(\mu)$. In the non-refractive case, we have $I_\nu(\tau_\nu = 0, \mu = 0)/I_\nu(0, 1) = 0.423$ for $\lambda = 0.948 \mu\text{m}$. When refraction is introduced, the limb darkening is much weaker and $I_\nu(0, 0)/I_\nu(0, 1) = 0.947$. In the presence of refraction, ray paths that emerge with $\mu \sim 0$

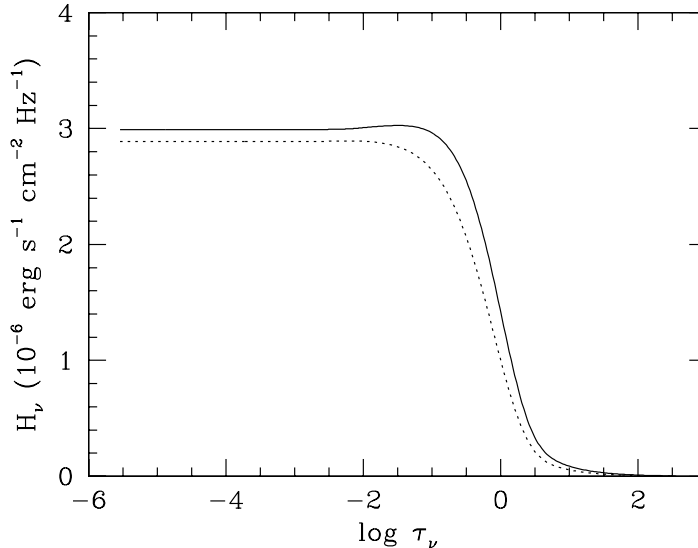


Fig. 6.— Radiative flux for refractive (solid line) and non-refractive (dotted line) cases as a function of vertical optical depth in the nominal white dwarf atmosphere model for $\lambda = 0.948 \mu\text{m}$. The atmospheric structure is the same for both calculations.

have been strongly deflected. The vertical optical depth τ_ν for a ray path exiting with $\mu = 0$ is related to σ_ν by

$$\tau_\nu = \int_0^{\sigma_\nu} \sqrt{1 - 1/n_\nu^2(\sigma'_\nu)} d\sigma'_\nu. \quad (63)$$

For $n_\nu(\tau_\nu)$ shown in Fig. 1 and $\sigma_\nu = 1$, we get $\tau_\nu = 0.56$. This means that due to refraction, a horizontal viewing angle allows us to see as deep inside the atmosphere as under angle $\mu = 0.56$ in the non-refractive case. We can indeed see on Fig. 6 that $I'_\nu(0, 0)_{\text{ref}} = I'_\nu(0, 0.56)_{\text{non ref}}$.

Despite the significant change in the specific intensity shown in Fig. 5, the radiative fluxes are nearly identical throughout the atmosphere (Fig. 6). This happens because in the absence of absorption and emission, refraction is a geometric effect that does not affect the value of the integral (16). By symmetry, the reflected ray paths do not contribute to the flux ($I'_\nu(+\mu) = I'_\nu(-\mu)$) and Snell's law implies that $n_\nu^2 \mu d\mu$ is constant. For reflected ray paths in an actual atmosphere, $I'_\nu(\tau_\nu, \mu > 0) > I'_\nu(\tau_\nu, \mu < 0)$, as emission is usually larger deeper inside the atmosphere and absorption processes are present. This explains why the radiative flux H_ν is slightly larger in the refractive case. For $\tau_\nu > 0.1$, the radiative flux decreases rapidly due to the presence of a convective zone, a characteristic of all cool white

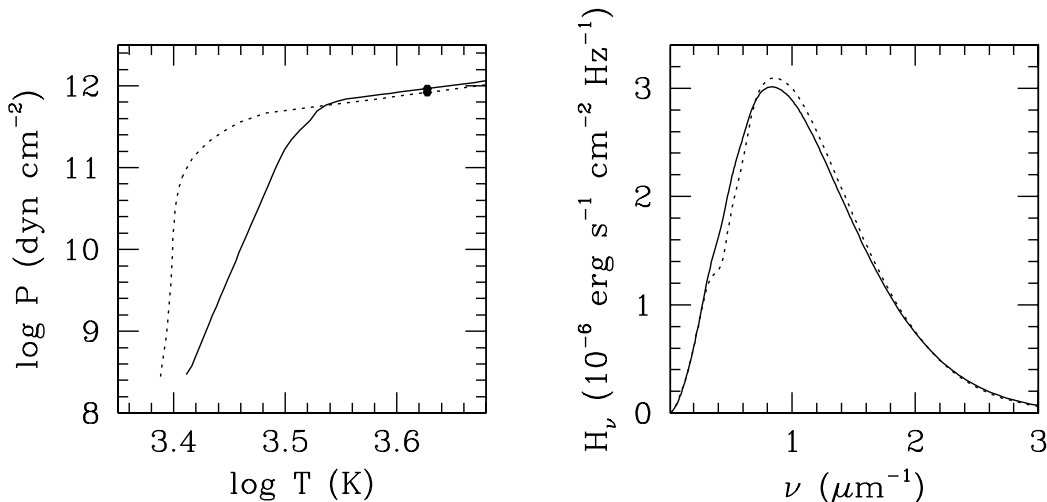


Fig. 7.— Pressure-temperature structure (left panel) and synthetic spectrum (right panel) for the nominal white dwarf atmosphere model parameters with (solid line) and without (dotted line) dispersive effects. Both models are computed by imposing flux conservation and hydrostatic equilibrium. The filled circle indicates the level where the Rosseland mean optical depth $\tau_R = 1$.

dwarf atmospheres models.

So far, our discussion of the effects of refraction on the radiation field was based on a fixed (non-refractive) atmospheric pressure-temperature structure. A full atmosphere calculation consists of finding the structure that satisfy the equations of 1) radiative transfer, 2) flux constancy in convection zones and radiative equilibrium in radiative zones, and 3) hydrostatic equilibrium.¹ Figure 7 compares such a self-consistent calculation for both the non-refractive (nominal structure) and the refractive cases. As expected, internal reflection leads to a hotter structure near the surface. The spectra resulting from these self-consistent structures are shown in Fig. 7. The $0.4\mu\text{m}^{-1}$ feature seen in the non-refractive case is caused by collision-induced absorption (CIA) by the small amount of H_2 molecules present in this model ($n(\text{H}_2)/n(\text{He}) \sim 4 \times 10^{-7}$). In the refractive case, the hotter structure results in the dissociation of H_2 and reduces the CIA absorption. The effects of refraction become much

¹The atmosphere model uses a realistic helium equation of state which predicts a very low degree of ionization. Electron conduction in the atmosphere is therefore negligible (Bergeron et al. 1995), in contrast with the models of Kapranidis (1983).

larger in models with lower effective temperatures or higher gravities and generally decreases as the hydrogen abundance increases. A detailed study of refractive effects in very cool white dwarfs atmospheres and spectra will be the subject of a subsequent publication.

6. Conclusions

Having realized that in the dense atmospheres of very cool white dwarf stars – especially those with a composition dominated by helium – the index of refraction departs significantly from unity, we have solved the problem of radiative transfer in plane parallel, LTE, static stellar atmospheres in the presence of refraction for arbitrary vertical variations of the opacity, temperature, and index of refraction. We show how to modify the Feautrier solution and the Λ -iteration method to solve the equation of radiative transfer in the presence of refraction. The resulting methods are general and can be applied to any one-dimensional problem. For cool white dwarfs, the most important effect of refraction on the propagation of radiation in a dispersive medium is total internal reflection. This increases the mean intensity in the optically thin region near the surface, where the dispersive effects are strongest. If radiative equilibrium is imposed, this results in higher surface temperatures than in the non-refractive case. We also find that limb darkening is dramatically reduced by refraction. This first solution of the radiative transfer equation with dispersive effects in stellar atmospheres suggest that refraction is an important effect that must be considered when modeling the atmospheres of very cool white dwarfs.

The authors wish to thank D. Mihalas and L.H. Auer for useful discussions. P. Kowalski is grateful to the Los Alamos National Laboratory for its hospitality and support. The research presented here was supported by NSF grant AST97-31438, NASA grant NAG5-8906, and by the United States Department of Energy under contract W-7405-ENG-36.

REFERENCES

- Abdallah, P. B., & Dez, V. L. 2000, JQSRT, 65, 595
- Bergeron, P., Saumon, D., & Wesemael, F. 1995, ApJ, 65, 595.
- Cannon, C. J. 1973, AJ, 185, 621
- Cox, J. P., & Giuli, R. T. 1968, Principles of stellar structure, Vol. 1 (New York: Gordon and Breach), Chap. 2.
- Harris, E. G. 1965, Phys. Rev., 138, B479
- Hauschildt, P. H. 1992, JQSRT, 47, 6, 433
- Hauschildt, P. H., Storzer, H., & Baron, E. 1993, JQSRT, 51, 6, 875
- Huang, Y., Xia, X., & Tan, H. 2003, Numerical Heat Transfer Part B, 44, 83
- Kapranidis, S. 1983, ApJ, 275, 342
- Mihalas, D. 1978, Stellar Atmospheres (San Francisco: W. H. Freeman)
- Olson, G. L., Auer, & L. H., Buchler, J. R. 1986, JQSRT, 35, 6, 431
- Olson, G.L., & Kunasz, P.B. 1987, JQSRT, 38, 5, 325
- Pomranin, G. C. 1968, ApJ, 153, 321
- Zheleznyakov, V. V. 1967, ApJ, 148, 849